Available online at www.sciencedirect.com

SCIENCE DIRECT

Thin Solid Films 493 (2005) 152 – 159

www.elsevier.com/locate/tsf

Effects of pretreatment by ion implantation and interlayer on adhesion between aluminum substrate and TiN film

Youming Liu [a,c], Liuhe Li [a,b], Xun Cai [a,*], Qiulong Chen [a], Ming Xu [a], Yawei Hu [a]
Tik-Lam Cheung [c], C.H. Shek [c], Paul K. Chu [c,*]

[a] School of Materials Science and Engineering, Shanghai Jiaotong University, Shanghai 200030, PR China
[b] 702 Department, Mechanical Engineering School of Beijing, University of Aeronautic and Astronautic, Beijing 100083, PR China
[c] Department of Physics and Materials Science, City University of Hong Kong, Tat Chee Avenue, Kowloon, Hong Kong

Received 12 October 2004; received in revised form 9 February 2005; accepted 21 June 2005
Available online 28 September 2005

Abstract

Pretreatment of the aluminum substrate, such as Ti and Ni–P interlayer, can improve the adhesion strength and mechanical properties of deposited TiN films. In this work, in order to compare with the effect of Ti interlayer and Ni–P interlayer, aluminum substrate was pretreated by titanium ion implantation prior to the deposition of TiN films by magnetron sputtering in a custom-designed multifunctional ion implanter. A scratch tester was used to assess the coating adhesion by investigating the critical load, L_c, at which delamination or other types of coating failures take place. The effects of different pretreatments on the adhesion strength between the films and substrates were analyzed. Our experimental results show that all the adopted pretreatment approaches can effectively improve the adhesion of TiN coatings on aluminum but the failure modes are different for the different coatings/substrate systems. Among the different processes, the use of a thick Ni–P interlayer (10 μm) and Ti ion implantation together with a Ti interlayer (300 nm) produce the better effects, as the adhesion strength increases from 0.7 to 3.7 and 4.0 N, respectively.

PACS: 68.35.G
Keywords: Titanium nitride; Implantation; Adhesion; Acoustic emission

1. Introduction

Because of the good wear and corrosion resistance, TiN has become one of the most attractive materials used to improve the friction and wear performance of tool surface. It is widely recognized that the substrate plays an important role in determining the mechanical properties and wear resistance of the coatings. Usually, hard steels are used as the substrate materials because of their good loading capacity, as has been widely studied [1–5]. However, there are many applications in which the coatings are deposited on substrates with lower hardness or stiffness values (such as aluminum and its alloys) than conventional hard tool-steel substrates. There have hitherto not been many studies about hard coatings deposited on aluminum substrate. Marlaczynski and Hamdi [6] determined the feasibility of surface modification to improve the tribological properties of highly eutectic aluminum alloys. Plasma immersion ion implantation was developed to produce diamond-like hydrocarbon coatings on aluminum 390 alloy. Mukherjee et al. [7] also employed plasma immersion ion implantation and deposition technology to deposit TiN coatings on Al substrate.

The coating lifetime depends greatly on the adhesion between the coating and substrate [8–10]. Conventionally, it is accomplished by the deposition of a Ti interlayer on the substrate before the TiN coating is deposited. Here, we propose a different method by using Ti ion implantation,

* Corresponding authors. Xun Cai is to be contacted at Tel.: +86 21 62932087; fax: +86 21 62932587. Paul K. Chu, Tel.: +852 27887724; fax: +852 27889549.
E-mail addresses: xcai@sjtu.du.cn (X. Cai), paul.chu@cityu.edu.hk (P.K. Chu).

0040-6090/$ - see front matter © 2005 Published by Elsevier B.V.
doi:10.1016/j.tsf.2005.06.045

Ti and Ni–P interlayer to generate a gradient layer that can spread the stress gradually prior to the deposition TiN film. Nitrogen and titanium ion implantation have been proposed for surface modification of aluminum and steel [11–13]. These pretreatment steps are expected to enhance the bonding between TiN and Al thereby improving the resistance against larger loading and plastic deformation as well as enhancing the adhesion strength. In our process, a strengthening layer is formed and previous studies have shown that the nanohardness and frictional properties of aluminum can be improved. The critical load, L_c, for coating failure is normally assessed by microscopic examination of the track after a scratch has been made or by the onset of acoustic emission as coating spalls occur [14]. Dyrda and Sayer [15] have suggested an effective friction coefficient $\mu = F_H/F_N$ as a measure of the critical load, where F_H is the horizontal force required to move the sample under the indenter under a normal force F_N. In this study, we employ microscopic examination, acoustic emission and friction coefficients to more accurately determine the critical load L_c.

2. Experimental details

2.1. Specimen preparation

Samples with dimensions of $15 \times 15 \times 5$ mm made of pure aluminum (99.99%) were used in our experiments. The specimens were mechanically polished and ultrasonically cleaned in isopropyl alcohol for about 10 min prior to implantation. Ion implantation was conducted in a custom-designed multifunctional ion implanter schematically depicted in Fig. 1. The instrument is equipped with a direct current magnetron sputtering source, a metal vapor vacuum arc and a Kaufman ion implantation source in the same vacuum chamber. The sample temperature during implantation was measured by a thermocouple mounted on

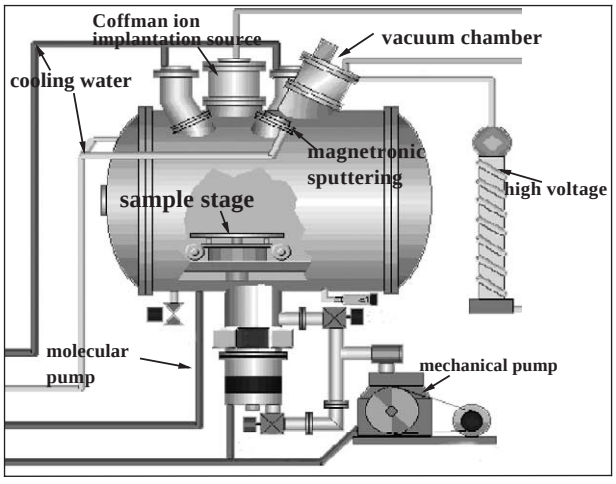

Fig. 1. Schematic of the custom-designed multifunctional ion implanter.

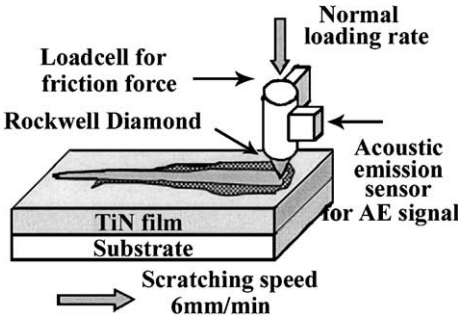

Fig. 2. Schematic diagram of the scratch tester.

the sample holder and a pyrometer installed in the vacuum chamber. No external heating was applied to the specimen and so any temperature increase was due to the incident ion beam and magnetron sputtering. The sample was implanted with 40 keV Ti ion to a dose of 2×10^{17} ions/cm^{-2}. The ion beam current density was about 25 μA/cm^2. The aluminum substrates with Ni–P interlayers were supplied by Kaifa Company. The Ni–P coating was produced by chemical plating technology and its thickness was 10 μm.

After implantation, the sample was rotated to face the magnetron sputtering target without breaking vacuum. The background pressure in the deposition chamber was less than 2×10^{-3} Pa. The distance between the sample and magnetron sputtering source was about 4 to 5 cm. The target was made of 99.4% pure titanium, and the target voltage and current were 420 V and 1.0 A, respectively. The nitrogen and argon gases were 99.99% pure, and the total pressure and N_2 partial pressure were 3.0×10^{-1} and 5.0×10^{-2} Pa, respectively. The negative sample bias voltage was −60 V. The thickness of the films was determined by profilometry. The deposition rates of the TiN and Ti films were calculated to be ~0.47 nm/s and ~0.5 nm/s, respectively. The TiN films on all samples were about 1.7 μm thick and that of the Ti interlayer was about 150 nm. The nanohardness of the films was determined using a nanoindentation tester (CSEM Instruments). The scanning electronic microscope (SEM) images depicting the interfaces of the TiN/Al/Ti and TiN/Ti/Ti^+-implanted Al were obtained on a JEOL JSM-6335.

2.2. Scratch test

The normal radius of the Rockwell-shaped diamond indenter is 200 μm, but the minimum normal load usually begins from 1 N. Ashrafizadeh [16] reported that the adhesion strength (critical load) of PVD TiN coatings deposited on aluminum substrate was less than 1 N, and a 120° scratch indenter was used in his work. In our experiments, a scratch test apparatus (CSEM Instruments) with a Rockwell-shaped diamond indenter of 50 μm radius was used. The schematic diagram of the scratch tester is shown in Fig. 2. The tests were performed based on continuous loading with a normal force, F_N, from 0.5 to

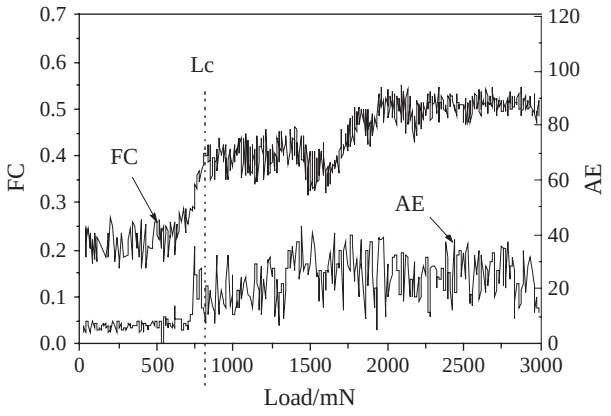

Fig. 3. Scratch test results of the TiN/Al sample.

10 N. The samples were scratched by increasing the normal load at a rate of 7477.5 mN/min and using a scratching speed of 6 mm/min for a distance of 8 mm. The friction coefficient F_C, and the acoustic emission signals A_E were recorded. A_E is constituted by elastic waves generated by the sudden crack in materials when external load is applied. The following test parameters were deduced from the scratch test:

(a) Critical load deduced from microscopic evaluation of the crack pattern around the scratch channel;
(b) Critical load deduced from friction coefficient along the scratch;
(c) Critical load deduced from the acoustic emission signal along the scratch.

3. Results

3.1. Characteristic FC of TiN/Al, TiN/Ti+-implanted Al and TiN/Ti/Al

Figs. 3–5 show that the effective F_C are almost constant under small loads but vary significantly under larger loads. The friction coefficient is $\mu = F_H/F_N$, where F_H is the horizontal force required to move the sample under the indenter under a normal force F_N. The irregular behavior observed for the friction coefficient is probably caused by chipping of the coating because of the extraordinarily soft aluminum substrate. The results are confirmed by A_E and microphotographs of the scratch channels in order to identify the onset of delamination or cracking. The fluctuation in A_E is in good agreement with the F_C data. A_E in Fig. 5 seems more fluctuant than that in Figs. 3 and 4 because of the different sensitivity setting. The average critical load value can be derived from the scratch tests. Our results show that critical load of the TiN coating on unimplanted Al substrate is 0.7 N. After substrate has been pretreated by Ti^+ implantation, the critical load increases to about 1.8 N. Critical load of TiN/Ti/Al is about 1.6 N.

3.2. Characteristic FC of TiN/Ti/Ti+-implanted Al and TiN/Ni–P/Al

The typical F_C and A_E diagrams are shown in Figs. 6 and 7, which demonstrate a transition in the slope. The (a), (b) and (c) micrographs correspond to region a, b and c, respectively. It can be argued [15] that the simplest approach for assessment of adhesion is to initially plot the F_C versus the normal force F_N. In this work, the intersecting point of the two different slopes of F_C is known as the critical load L_c. The materials response can be classified into the following three distinct regions.

Region a) F_C is low since the indenter moves on top of the coating and only plastic deformation occurs with no or few cracks, which are shown in Figs. 6(a) and 7(a). The surface and asperities are deformed into a smooth, polished intermediate film, and acoustic emission is either very low or does not exit. As the load increases, the indenter penetrates deeper and hardening of the films and regular cracks hinder the movement of the indenter. Therefore, F_C increases rapidly.

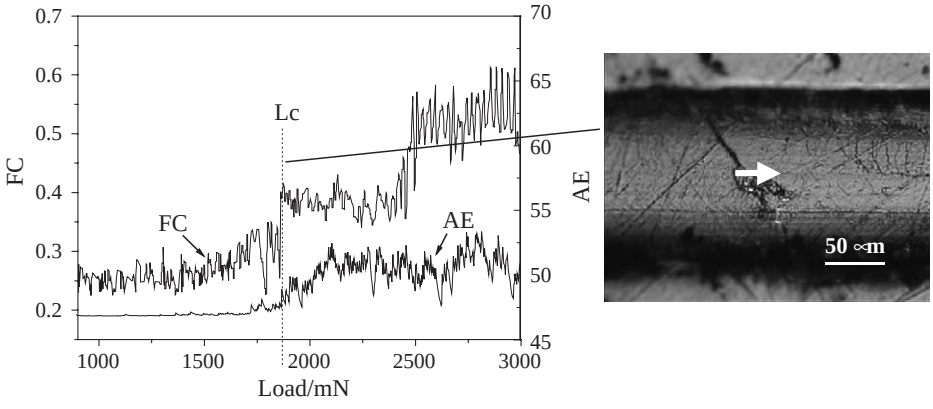

Fig. 4. Scratch test results of the TiN/Ti^+-implanted Al sample. The arrows indicate the sliding direction.

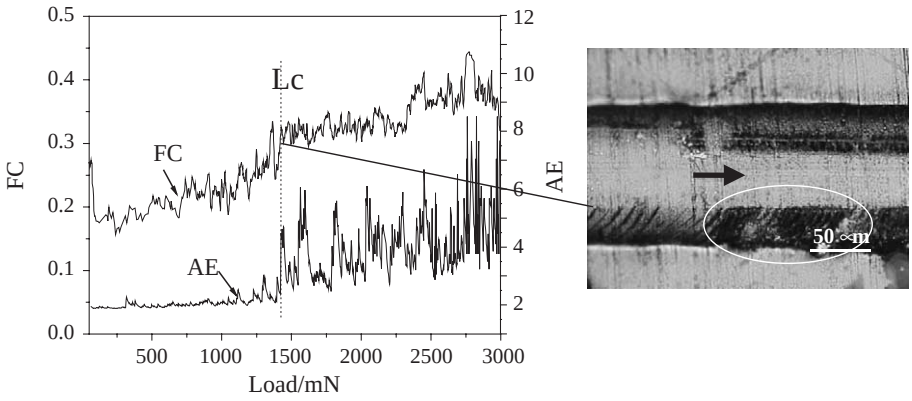

Fig. 5. Scratch test results of the TiN/Ti/Al sample.

Region b) This region is a transitional region. In this region, the interface cohesive stress is exceeded, but the internal energy is sufficient only to propagate circular cracks ahead of the indenter, and the transverse crack develops into a regular crack pattern just before coating failure at the critical load, which is verified by the microphotographs in Figs. 6(b) and 7(b). A_E begins to increase slightly before the critical load (L_c) for coating crack. F_C continues to increase due to the fracture energy absorbed in the substrate as the indenter ploughs.

Region c) The higher load-section provides information about the bulk properties of the coating and substrate. The softer aluminum substrate offers less resistance to indenter penetration. The ascending tendency of horizontal force (F_H) moving the sample under indenter decreases. Hence, the slope of F_C in the higher load-section is lower than that in the initial region. At the beginning of this region, A_E suddenly increase due to the cracking and fracture in coating. It may be argued that region c is the most important. With increasing loading, the indenter penetrates more deeply into the substrate. Adhesion is good as the applied mechanical energy is absorbed by extensive transverse cracking. The more extended this

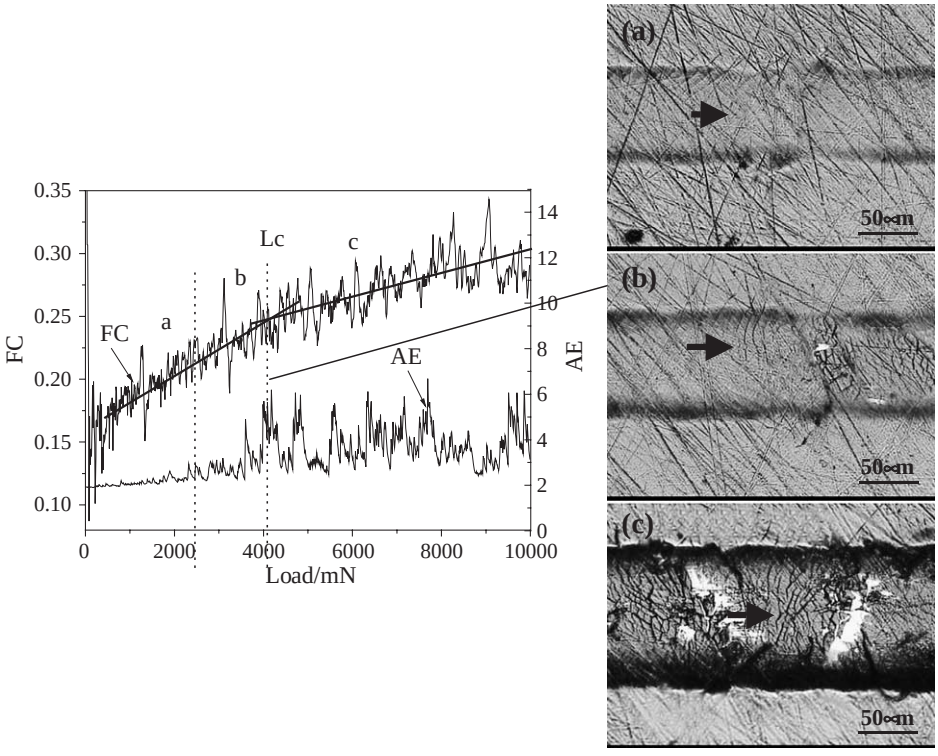

Fig. 6. Scratch test results of the TiN/Ti/Ti$^+$-implanted Al sample.

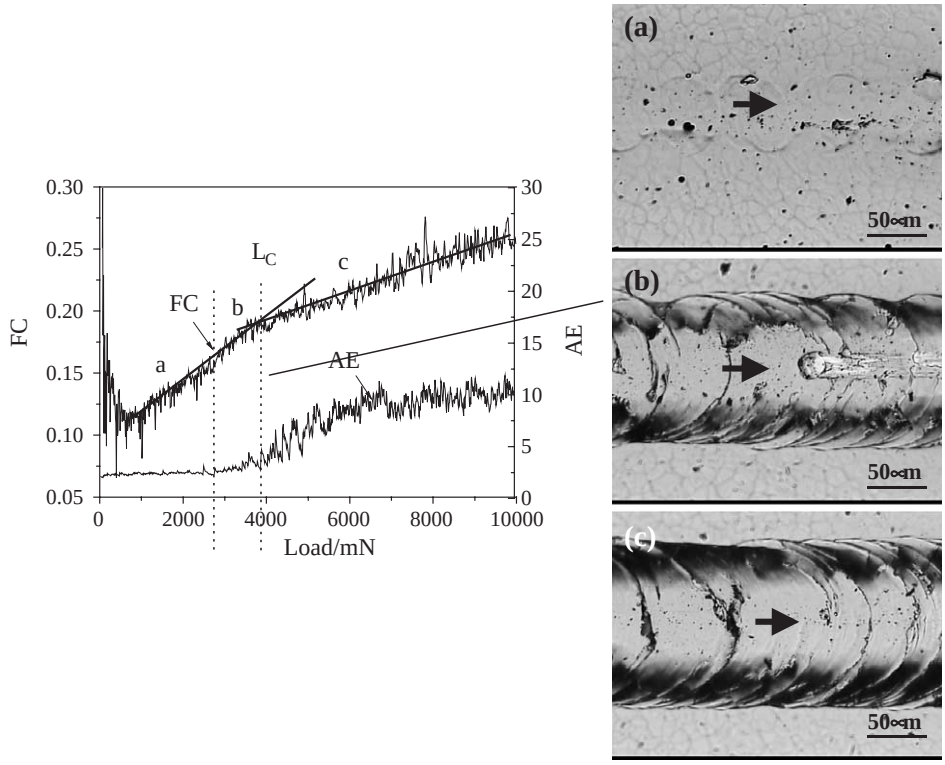

Fig. 7. Scratch test results of the TiN/Ni–P/Al sample.

region is, the better the coating adheres. When adhesion is not good, the coatings are removed from the substrate, and it is known as flaking failure. At the beginning of region c, A_E increases suddenly, which agrees well with the critical load L_c determined from F_C.

Actually, in some cases, the variations in the slope corresponding to different stages in deformation of TiN coating are not obvious and hence, the assessment of the critical load for coating failure is very complicated. Therefore, it needs to incorporate F_C, A_E and microphotographs of scratch when determining L_c. The adhesion strength of TiN/Ti/Ti$^+$-implanted Al and TiN/Ni–P/Al are about 4.0 and 3.7 N, respectively.

3.3. Failure modes

If the scratch test is to be used for the assessment of coating-substrate adhesion, then the adhesion-related failure modes are most important [17] (Fig. 8). A range of well-defined failure modes are shown in Fig. 9. The failure

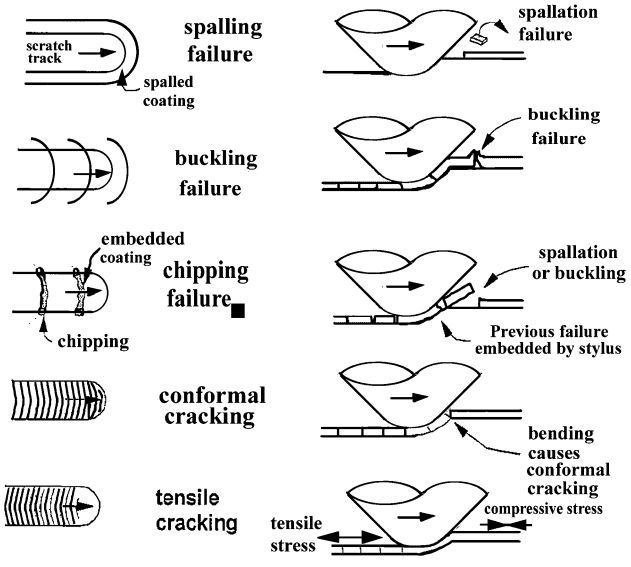

Fig. 8. Failure modes as described by Xie and Hawthorne [18].

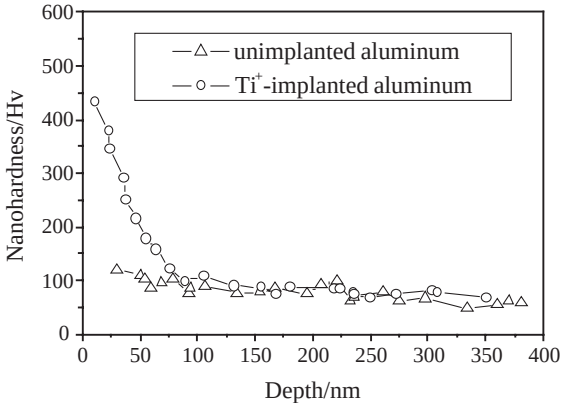

Fig. 9. Nanohardness of Ti$^+$-implanted aluminum and unimplanted aluminum as a function of the indentation depth.

modes in the scratch test of hard coatings can broadly be split into three categories:

1. Through-thickness cracking — including tensile cracking behind the indenter, conformal cracking as the coating is bent into the scratch track, and Hertzian cracking.
2. Spallation — including compressive spallation ahead of the indenter, buckling spallation ahead of the indenter, or elastic recovery induced spallation behind the indenter.
3. Chipping in the coating (akin to lateral cracking in bulk ceramics).

Generally, the critical load at which a given failure mode first occurs or occurs regularly along the scratch track is used as a method of coating adhesion assessment. Different failure modes reflect the adhesion strength of thin films and substrate.

Microscopic investigations shown in Figs. 4–7 confirm that different pretreatments of substrate result in different failure modes in our scratch test. The micrographs in Figs. 4 and 5 show that the bottom of the scratch channel is smooth, but buckling and chipping occur at the edge of the scratch channel. Xie and Hawthorne [18] suggest that the most familiar failure during scratch testing are 'sidewards parallel flaking' and 'sidewards lateral flaking' at scratch sides for a hard, thin coating-soft substrate system. The scratch indenter displaces the aluminum substrate form the bottom to the sides of groove during scratch test. Therefore, the coating is subjected to a bending deformation. The stress concentrates in the edge of the scratch due to the difference in the properties between TiN and aluminum, and hence, the TiN film in this region tends to buckle and crack. For the TiN/Ti^+-implanted Al system, the thickness of the enhancement layer is quite small (about 100 nm). For TiN/Ti/Al, although the aluminum substrate is strengthened by 300 nm of Ti interlayer, it is not cleaned by ion bombardment. Thus, the poor interface between substrate and Ti interlayer leads to earlier failure. We can conclude that the failure mode of TiN/Al, TiN/Ti^+-implanted Al and TiN/Ti/Al system are spallation failure.

The micrographs in Fig. 6 show that the failure mode of TiN/Ti/Ti^+-implanted Al belongs to tensile cracking. Tensile cracking occurs when the coating remains fully adherent. The failure mode of TiN/Ni–P/Al is the typical conformal failure which is shown in Fig. 7(b) and (c). The conformal failure mode only consists of cracking within the scratch; the cracks follow semicircular trajectories parallel to the leading edge of the indenter. These form as the indenter deforms the coating and the underlying substrate, resulting in tensile bending moments within the coating as it is pushed down underneath the indenter. While the tensile cracking failure mode appears superficially similar to the conformal cracking described above, the semicircular cracks are now parallel to the trailing edge of the indenter. These cracks form as a result of the tensile frictional stresses present behind the trailing edge of the stylus and these stresses balance the compressive frictional stress ahead. The changed failure modes are believed to be caused by enhanced adhesion of film on substrate and enhanced load-capacity of substrate, which will be discussed in the following paragraphs.

4. Discussion

It is generally recognized that the substrate plays an important role in determining the mechanical properties and wear resistance of the coatings. For hard TiN films on soft aluminum substrate, the large variation in the coefficient of thermal expansion and mechanical properties between the TiN film and aluminum substrate will result in large residual stress. Meanwhile, the bombardment of Ar atoms during sputtering also could cause intrinsic stresses in sputter-deposited films [19]. Therefore, the TiN/Al system suffers earlier failure during scratch test.

Rickerby et al. [20] suggest that substrate with higher hardness could provide a more effective support for the TiN film and thus the critical load increases. In this work, after Ti ion implantation, the surface hardness of the aluminum substrate goes up from 100 to 440 HV as shown in Fig. 9.

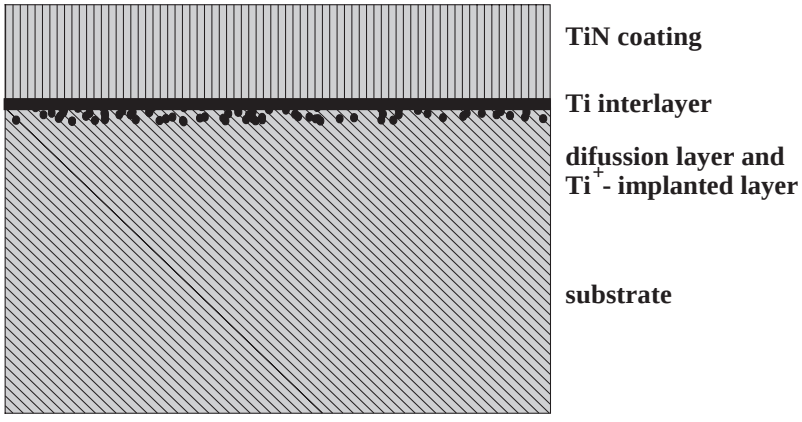

Fig. 10. Schematic of TiN/Ti/Ti^+-implanted Al.

The titanium atoms exhibit a Gaussian distribution and a surface layer with graded hardness is formed [11–13]. Although Young's moduli E of TiN and soft aluminum substrate are quite different, the enhanced gradient layer with higher hardness can reduce stress concentration in the whole system, especially at the interface [21]. As a result, the loading capacity and resistance to plastic deformation are improved and then the adhesion strength of TiN films on ion-implanted aluminum is increased. Obviously, the 10 μm thick Ni–P can further improve the load capacity and resistance to plastic deformation than that of ion implantation substrate and thinner Ti interlayer, so the adhesion strength also increases to about 3.8 N.

Compared to the TiN/Ti/Al system, the adhesion strength of the TiN/Ti/Ti^+-implanted Al system may be further improved by interdiffusion between Ti interlayer and Ti^+-implanted aluminum substrate. Travessa et. al. [22] have suggested that a Ti interlayer joins easily to both ceramic and steel parts. However, diffusion must be conducted between 500 and 800 °C, which is not suitable for aluminum with a low melting point. High energy titanium ion implantation together with a Ti interlayer may be an alternative method to improve adhesion between TiN film and aluminum substrate. For the TiN/Ti/Ti^+-implanted Al, the aluminum substrate is heated by ion bombardment while there is no sample cooling mechanism. Hence, the processing temperature of the TiN/Ti/T^+-implanted Al system is higher than that of the TiN/Ti/-unimplanted Al system. A higher temperature can improve the interdiffusion of films and substrate. Therefore, adhesion between the TiN film and Ti^+-implanted aluminum substrate is improved. Refs. [23, 24] also reported that heating of the substrate during ion implantation could improve the adhesion strength between the TiN film and substrate. A schematic of adhesion strengthening in the TiN/Ti/Ti^+-implanted Al sample is shown in Fig. 10. In addition, during ion implantation, surface contaminants and the surface oxide film on the aluminum substrate decrease the adhesion strength, and high energy ion implantation causes radiation damages to the substrate surface that may be beneficial to nucleation. These explanations also can be applied to TiN/ Ti^+-implanted Al system. Fig. 11 shows the cross sectional SEM images of the TiN/Ti/Al and TiN/Ti/Ti^+-implanted/Al samples. The interface of the TiN/Ti/Ti^+-implanted Al sample is smoother and denser than the TiN/Ti/-unimplanted Al sample. Consequently, better adhesion is expected.

5. Conclusions

Pretreatment of the aluminum substrate by means of Ti^+ implantation, Ti interlayer and Ni–P interlayer can effectively improve the adhesion strength of deposited TiN films. A thick Ni–P interlayer (10 μm) and a combination of T^+ implantation and Ti interlayer (300 nm) exhibit the best effects. The adhesion strength increases from 0.7 N (TiN/Al) to 3.7 N (TiN/Ni–P/Al) and 4.0 N (TiN/Ti/Ti^+-implanted Al), respectively. During the scratch test, the combination of F_C, A_E and microphotographs of scratch channel more accurately determine the critical load of the TiN films at which delamination or other types of coating failure take place. Irregular F_C values are observed in the TiN/Al, TiN/ Ti^+-implanted Al and TiN/Ti/Al samples, and a transition in the slope of the F_C trend is observed in the TiN/Ni–P/Al and TiN/Ti/Ti^+-implanted Al samples. Different failure modes are observed for different pretreatments using the scratch test.

Acknowledgements

This work was supported by National Natural Science Foundation of China No. 50271004, Hong Kong Research Grants Council (RGC) Competitive Earmarked Research Grant (CERG) No. City U1137/03E, City University of Hong Kong Strategic Research Grant (SRG) No. 7001642

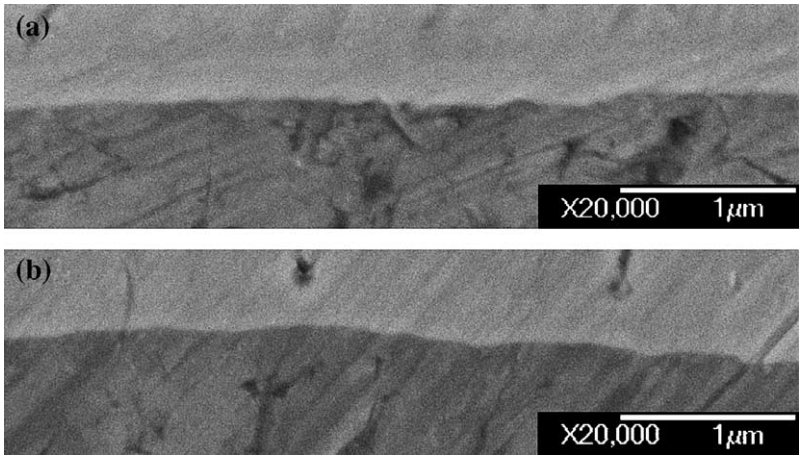

Fig. 11. SEM images of interface of TiN/Al/Ti and TiN/Ti/Ti^+-implanted Al. (a): TiN/Ti/Al; (b)TiN/Ti/ Ti^+-implanted Al.

and Scientific Effort of Shanghai Science and Technology Committee 0359 nm 005.

References

[1] B.W. Karr, I. Petrov, D.G. Cahill, J.E. Greene, Appl. Phys. Lett. 70 (1997) 1703.
[2] F.S. Shieu, L.H. Cheng, Y.C. Sung, Mater. Chem. Phys. 50 (1997) 248.
[3] Q. Fang, J.Y. Zhang, Int. J. Inorg. Mater. 3 (2001) 1193.
[4] J. Michalski, E. Lunarska, T. Wierzchon, S. AlGhanem, Surf. Coat. Technol. 72 (1995) 189.
[5] B.K. Tay, X. Shi, H.S. Yang, Surf. Coat. Technol. 111 (1999) 229.
[6] G.W. Marlaczynski, A.H. Hamdi, Surf. Coat. Technol. 93 (1997) 280.
[7] S. Mukherjee, F. Prokert, E. Richter, W. Möller, Thin Solid Films 445 (2003) 48.
[8] N. Dilawar, R. Kapil, Brahamprakash, Thin Solid Films 323 (1998) 163.
[9] Q.H. Fan, J. Grácio, N. Ali, E. Pereira, Diamond Relat. Mater. 10 (2001) 797.
[10] K.R. Lee, K.Y. Eun, I. Kim, J. Kim, Thin Solid Films 377–378 (2000) 261.
[11] J. Jagielskia, A. Piatkowska, P. Aubert, C. Legrand-Buscema, Vacuum 70 (2003) 147.
[12] J. Chakraborty, S. Mukherjee, P.M. Raole, P.I. John, Mater. Sci. Eng. A304–A306 (2001) 910.
[13] S.T. Knight, P.J. Evans, M. Samandi, Nucl. Instrum. Methods Phys. Res., B 119 (1996) 501.
[14] H. Jensen, U.M. Jensen, G. Sorensen, Surf. Coat. Technol. 74–75 (1995) 297.
[15] K. Dyrda, M. Sayer, Thin Solid Films 355–356 (1999) 277.
[16] F. Ashrafizadeh, Surf. Coat. Technol. 130 (2000) 183.
[17] S.J. Bull, Tribol. Int. 30 (1997) 491.
[18] Y. Xie, H.M. Hawthorne, Surf. Coat. Technol. 155 (2002) 121.
[19] S. Ulrich, H. Ehrhardt, J. Schwan, R. Samlenski, R. Brenn, Diamond Relat. Mater. 7 (1998) 835.
[20] D.S. Rickerby, S.J. Bull, T. Robertson, A. Hendry, Surf. Coat. Technol. (1990) 63.
[21] G.S. Kim, S.Y. Lee, J.H. Hahn, B.Y. Lee, J.G. Han, J.H. Lee, S.Y. Lee, Surf. Coat. Technol. 171 (2003) 83.
[22] D. Travessa, M. Ferrante, G. Den Ouden, Mater. Sci. Eng. A337 (2002) 287.
[23] I.A. Solodukhin, V.V. Khodasevicha, Surf. Coat. Technol. 142–144 (2001) 1144.
[24] U.H. Hwang, Thin solid films 254 (1995) 16.